Simulation of the magnetoresistance of Heisenberg spin lattices using the resistor—network model

Simulation of the magnetoresistance of Heisenberg spin lattices using the resistor–network model*

Lin Ling-Fang(林玲芳), Huang Xin(黄 欣), and Dong Shuai(董 帅)†

Department of Physics, Southeast University, Nanjing 211189, *China*

(Received 7 April 2013; revised manuscript received 9 May 2013)

The magnetism and conductance of two-dimensional Heisenberg spin lattices are investigated by using Monte Carlo simulations to qualitatively understand a fascinating magnetoresistance effect observed in magnetic materials and their artificial multilayers. Various magnetic profiles, including a pure ferromagnetic, a pure antiferromagnetic, two phase competitive cases, and an artificial sandwich junction, are simulated, and their conductances are calculated based on an extended resistor–network model. Magnetoresistance is observed in some lattices, which is prominent when the system is near phase boundaries. Compared with real manganites, the absence of colossal magnetoresistance in our simulation implies the essential role of charge ordered phase which is not included in our pure spin model. However, our model provides an intuitive understanding of the spin-dependent conductance in large scale.

Keywords: magnetoresistance, resistor–network model, phase competition

PACS: 73.43.Qt, 75.10.Hk, 75.40.Mg **DOI:** 10.1088/1674-1056/22/11/117313

1. Introduction

Magnetoresistance (MR) has been extensively studied in the past two decades and continues to attract much research interest due to its high technical applications as well as its unusual physical importance.[1,2] On one hand, the discovery of giant MR (GMR) and tunneling MR (TMR) found in metallic multilayers and metal–insulator–metal multilayers has rendered widely used spintronic devices. On the other hand, the colossal MR (CMR) found in perovskite manganites and some other complex oxides provides a unique playground to study the complexity of strongly correlated electron systems.[3–5]

Regarding the MR effect in manganites, the underlying mechanism was firstly proposed as the double-exchange process.[6–8] However, further studies found that only double-exchange itself is not enough to understand the CMR effect.[9,10] A wide variety of theoretical investigations and experiments have shown the strong tendency of phase separation and percolative metal–insulator transition (MIT) in manganites.[3,11,12] Currently, it has been widely accepted that the competitions among various phases, e.g., ferromagnetic (FM) metallic phase and paramagnetic/antiferromagnetic (PM/AFM) insulating phases, lead to MIT and CMR effects.[5,13–15]

Recently, Şen *et al.* found the competing AFM phase in the CMR region is the CE-type antiferromagnet or its derivations.[16,17] Then, an interesting question is whether this particular CE-like phase is a prerequisite for CMR, or whether other AFM states play a similar role in the phase competitions. If so, then the CMR effect should not be restricted in manganites but also be possible in other materials with phase competitions. In this work, the phase competitions between FM state and G-type AFM state will be studied on Heisenberg spin lattices. This toy model can provide a simple but intuitive physical picture to clarify the relationship between MR and phase competitions.[18]

2. Model and method

The Heisenberg spin model on a square lattice ($L \times L$, $L = 36$) with periodic boundary conditions is adopted to describe a magnetic system. The model Hamiltonian reads

$$H = \sum_{<i,j>} J_{i,j} \boldsymbol{S}_i \cdot \boldsymbol{S}_j - \boldsymbol{S}_i \cdot \boldsymbol{h}, \tag{1}$$

where $J_{i,j}$ is the exchange interaction between the nearest-neighbor (NN) spins $\boldsymbol{S}_i$ and $\boldsymbol{S}_j$, $\boldsymbol{h}$ is the external magnetic field, and the length of spin is normalized as unit 1 in the following.

The standard Markov chain Monte Carlo (MC) method with the metropolis algorithm is employed to trace phase transitions. In our MC simulation, the first 1×10^4 MC steps (MCSs) are used for thermal equilibrium, then the following 1×10^4 MCSs are used for measurements. In all simulations, the acceptance ratio of MC updates is controlled to be about 50% by adjusting the updating windows for spin vectors. Total energies per site (E's) and specific heats per site ($C_{\rm v}(T)$'s) are measured as a function of temperature (T). The

*Project supported by the National Natural Science Foundation of China (Grant No. 11004027), the New Century Excellent Talents in University of China (Grant No. 10-0325), the Research Fund for the Doctoral Program of Higher Education of China (Grant No. 20100092120032), and the National Student Research Training Program (Grant No. 1310286044).

†Corresponding author. E-mail: sdong@seu.edu.cn

$C_v(T)$ is calculated using the standard fluctuation equation: $N(\langle E^2\rangle - \langle E\rangle^2)/k_B T^2$, where the Boltzmann constant k_B is taken as 1, N is the number of total sites, and $\langle\rangle$ denotes the MC average. To characterize the FM and AFM orders, the spin structure factors are calculated by[19,20]

$$S(\boldsymbol{k}) = \frac{1}{N^2}\sum_j \boldsymbol{S}_j \cdot \boldsymbol{S}_{j+\boldsymbol{r}} \exp[\mathrm{i}\boldsymbol{k}\cdot(j+\boldsymbol{r})], \tag{2}$$

where $\boldsymbol{r}$ and $\boldsymbol{k}$ are vectors in real and reciprocal spaces, respectively.

The Heisenberg spin model is a very general model for magnetic systems and can be modified to describe many particular materials. In the simplest case, $J_{i,j}$ is uniformly positive or negative, then the ground state of lattice is pure G-type AFM or FM. To address the phase competitions, two methods are used: 1) by introducing a random field,[21] e.g., random distributions of positive and negative $J_{i,j}$'s; 2) by adding one more competitive item into Eq. (1), e.g., a classical double-exchange item $-t\sqrt{1+\boldsymbol{S}_i\cdot\boldsymbol{S}_j}$, where t is the double-exchange coefficient.[22,23] The sketch of these lattices are shown in Fig. 1(a).

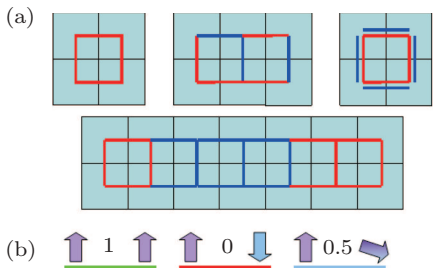

Fig. 1. (color online) (a) Schematic diagram of the 2D Heisenberg spin lattices. Upper: from left to right, the lattices are for a pure FM (or pure AFM) lattice, random-field lattice, and double-exchange frustrated lattice, respectively. Lower: an artificial sandwich junction. The red and blue bonds connecting NN grids represent different exchanges, e.g., J_+/J_- or t/J. (b) The sketch of local resistor based on NN spins. Left: when adjacent spins are parallel, the local conductance is maximal (1). Middle: when NN spins are antiparallel, the local conductance is 0. Right: for arbitrary spin pair, for example 120°, the local conductance can be calculated using $\sqrt{(1+\boldsymbol{S}_i\cdot\boldsymbol{S}_j)/2}$.

The conductances of the spin lattices are calculated by the resistor–network model.[21,24–28] A resistor is assigned between each NN site with a value: $C_{i,j} = \sqrt{(1+\boldsymbol{S}_i\cdot\boldsymbol{S}_j)/2}$, as shown in Fig. 1(b). Its physical meaning is that when adjacent spins are in the same direction, the conductance is maximum, and conversely when NN spins are antiparallel, the conductance is 0. This formula can describe a spin-dependent transport, e.g., the Kondo effect.[6,7] After building such a resistor network, the profile of local voltages and the total conductance (C_{rn}) of the resistor network are calculated by solving Kirchhoff's equations.[25]

In detail, a system of linear Kirchoff equations is constructed for each site, which reads

$$\sum_j C_{i,j}(V_i - V_j) = 0, \tag{3}$$

where i and j are NN sites; V_i and V_j are the voltages at sites i and j, respectively; $C_{i,j}$ are the conductances of local resistor between sites i and j, as calculated by the aforementioned equation. The summation is over all local NN's for each i.

The range of the total conductance C_{rn} is from 1 to 0, corresponding to the metallic and insulating limits, respectively. Then, the MR effect is calculated by: $[R(h)-R(0)]/R(0)$, where $R(h) = 1/C_{rn}(h)$ is the resistance of the network under the magnetic field h.

The present resistor–network model goes beyond previous studies.[21,24–28] In these previous models, two or three types of fixed resistors are used to construct the network, while in the current case all resistors depend on the correlation between Heisenberg spins, which is more realistic for spin-dependent transport.

3. Results and discussion

3.1. Pure FM and AFM lattices

First, the simplest cases (pure FM and AFM orders) are calculated. For simplicity, the value of $J_{i,j}$ is set to be uniform $J_- = -1$ and $J_+ = 1$ which corresponds to the FM and G-AFM ground states, respectively. As shown in Fig. 2(a), the specific heats and spin structure factors are shown as functions of T. Both of these two cases (FM, AFM) show identical T-dependent behaviors even though the ground magnetic states are different, e.g., both two $C_v(T)$ curves show peaks around $T = 0.7$, suggesting phase transitions. Correspondingly, the curves of spin structure factors also show transitions at the same T (the Curie temperature T_C and Néel temperature T_N), in agreement with the specific heats.

Then, the external magnetic field is switched on and the conductances are calculated. As summarized in Fig. 2(b), the resistances of FM and AFM lattices show divergent behaviors. In the AFM case, the resistance is entirely large and increases with decreasing T, suggesting an insulating behavior. By contrast, the resistance of FM lattice is small in the whole T range and decreases with decreasing T, implying a metallic behavior.

According to Figs. 2(c) and 2(d), it is obvious that the MR effect is prominent in the FM system (e.g., up to -7% at $T = 0.8$ under $h = 0.2$) in comparison with the AFM system (all below -2% under $h = 0.2$). Also, the MR in the FM case is most obvious at $T = 0.7$–0.9 especially under low magnetic fields. It shows us that the low-field MR effect is optimal in a T window a little higher than the PM–FM phase transition, which agrees with the experimental observation in wide-bandwidth manganites like $La_{0.7}Sr_{0.3}MnO_3$. The MR behavior in such a pure FM spin lattice, including its amplitude and optimal T range, is close to the so-called "CMR2" in Aliaga *et al*'s classification, of which amplitude is not really colossal.[13]

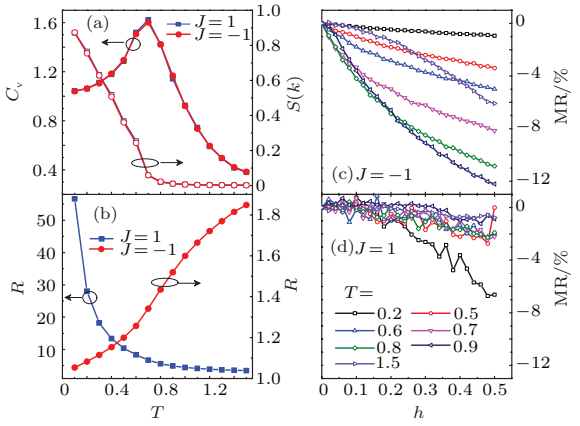

Fig. 2. (color online) MC results for the pure FM ($J=-1$) and AFM ($J=1$) lattices. (a) Specific heat (C_v) and the spin structure factor ($S(\boldsymbol{k})$) as a function of T. For the FM and AFM cases, the characteristic $\boldsymbol{k}$ are $(0,0)$ and (π,π), respectively. (b) Resistance. (c) and (d) MR as a function of the external magnetic field at different T's: (c) FM; (d) AFM. The fluctuation is large in the AFM case since the conductance $C_{\rm rn}$ of insulating lattice is nearly zero, which lowers the accuracy of resistance R.

3.2. Competitive FM+AFM lattices I: Random-field approximation

Although the pure FM lattice above has large MR near $T_{\rm C}$, the value of MR remains far from the colossal amplitude of real CMR effect. Şen *et al*'s simulations emphasized the phase competition between FM and AFM phases which is essential for CMR effect.[14,16] In our classical spin model, it is also possible to introduce phase competitions into the lattice. One of the simplest choices is to use a random-field approximation by using random exchanges $J_{i,j}$'s. In detail, $J_{i,j}$'s are randomly set as $J_+=+1$ or $J_-=-1$, and the ratio between FM and AMF phases is tuned to simulate different phase competitions. In practice, three kinds of ratio, $25\%J_-+75\%J_+$, $50\%J_-+50\%J_+$, and $75\%J_-+25\%J_+$, are adopted as the representatives of more AFM, half-half, and more FM competitive lattices.

By using this competing interactions, the most prominent MR appears in Fig. 3(c) with 75% FM exchange and 25% AFM exchange, while in other cases the MR effect is not so significant under low magnetic fields, although the $50\%J_-+50\%J_+$ case also shows a considerable MR under strong magnetic fields (see Fig. 3(b)). This contrast suggests that tiny doping of AFM components into FM background is advantage for the MR effect, while a mostly AFM lattice will make the insulating state very robust against the low external fields and thus suppress the MR effect.

Furthermore, the random field by doping with different J's suppresses the critical T's of phase transitions. For example, the phase transition for the $75\%J_-+25\%J_+$ case drops to $T=0.2$–0.3 (not shown here), which is much lower than 0.7 in the above pure FM case. However, as summarized in Fig. 3(d), the working T region with significant MR effect is enlarged ($T\leq 0.4$), compared with the narrow optimal T windows in the above pure FM case, which is a broadening of phase transition by the random-field disorder. The underlying physical mechanism, or more explicitly, the phase competition, is not the simple PM–FM one, but the more complex PM–AFM–FM one here.

3.3. Competitive FM+AFM lattices II: double-exchange exchange

There is more than one way to introduce competition into magnetic systems. Here, an alternative choice based on the exchange frustration is tested to avoid the random-field disorder effect. The frustration comes from the competition between two types of NN exchanges: superexchange $J_{i,j}$ ($=J>0$) and double-exchange t, as introduced in Section 2. Here, the double-exchange process is simplified into a classical expression as used by Landau *et al*,[22,23] which catches the intensity of double-exchange, but discards the Berry phase item. The double-exchange coefficient t is chosen as $\sqrt{2}$, while the superexchange J is adjusted to find a proper region of phase competition, similar to what Şen *et al*. did in the quantum version of double-exchange model.[14,16]

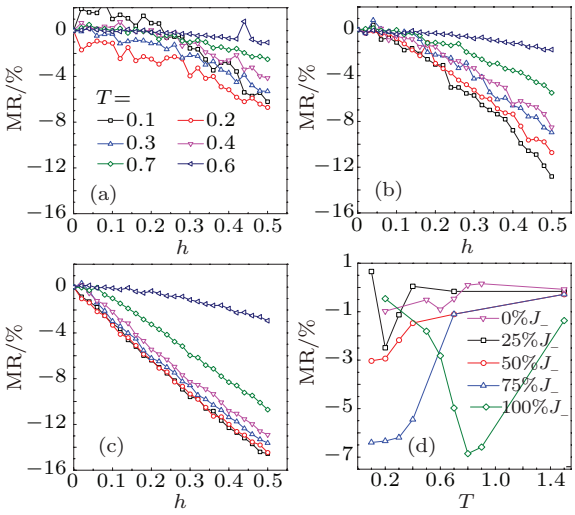

Fig. 3. (color online) MC results for competitive FM+AFM lattices with random-field approximation. (a) $25\%J_-+75\%J_+$; (b) $50\%J_-+50\%J_+$; (c) $75\%J_-+25\%J_+$; (d) summary of T-dependent MR at a low field ($h=0.2$) for different competitive lattices and pure FM/AFM cases. As mentioned above, the fluctuations of MR and resistance are large for insulating lattices.

Figure 4(a) shows the spin structure factors at a high $T=0.7$ and a low $T=0.2$, as a function of J. The $T=0.7$ corresponds to a high-T PM state without any prominent values of $S(\boldsymbol{k})$. In the low-T case, the FM order is clear with a large value of $S(0,0)$ when J is weak. However, this FM order becomes weaker and weaker with increasing J, characterized by deceasing value of $S(0,0)$. When $J=0.5$, the value of $S(0,0)$ is already very faint, implying the absence of long-range FM order at $T=0.2$. In the whole J range ($0\leq J\leq 1$) considered here, the AFM $S(\pi,\pi)$ are always faint, suggesting the absence of long-range AFM order.

In the following, we will only focus on the $J = 0.5$ case, which is taken as the example of competitive FM+AFM lattice. The T-dependent spin structure factors at $(0,0)$ and (π,π) are shown in Fig. 4(b). Although both values are not prominent, the FM one appears when T is low enough, e.g., $T = 0.1$, suggesting the weak FM tendency. By contrast, the AFM tendency is not observed here. The T-dependent resistance shows the metallic behavior (see Fig. 4(c)). The MR effect, as shown in Fig. 4(d), is considerable even when T is high, e.g., $T = 0.5$ or 0.7 which is far above T_C. Thus, in this competitive FM+AFM lattice, the MR working T window is also somewhat broadenedeven without the random-field disorder.

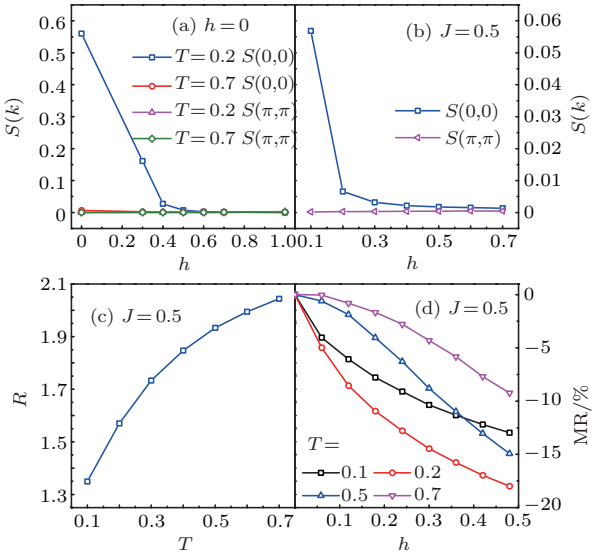

Fig. 4. (color online) MC results for the competitive FM+AFM lattices with the double-exchange coupling. (a) Spin structure factors at two typical T's as a function of T. (b)–(d) With a proper competing $J = 0.5$: (b) T-dependent conductance (left axis) and spin structure factor (right axis); (c) resistance as a function of T; (d) h-dependent MR at different T.

3.4. FM–AFM–FM sandwich junction

In the above simulations, the phase competition, which is important in bulk materials, is emphasized. It is also interesting to address the artificial sandwich structure, which is a common unit of spin-valve heterostructure.[29] In this sandwich junction, the insulating AFM layer is sandwiched between two conducting FM layers. In the Heisenberg spin lattice, this sandwich structure can be obtained by setting $J_{i,j}$ as $J_+ = +1$ in the AFM layers but $J_- = -1$ elsewhere. Here, we used an AFM bilayer inserted in the FM background.

Despite of the insertion of this AFM bilayer, the MC simulation shows a robust metallic FM order, as shown in Figs. 5(a)–5(c), which is similar to the aforementioned pure FM case (see Fig. 2) with a little lowered T_C. The MR shown in Fig. 5(d) is significant in a proper T range, which is also similar to the pure FM case.

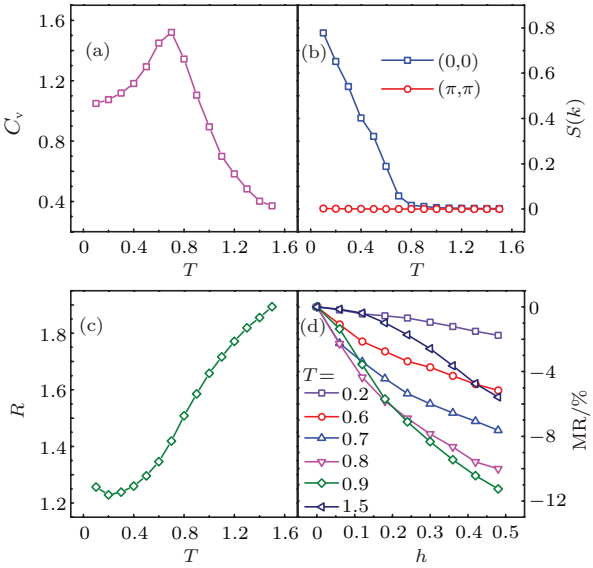

Fig. 5. (color online) MC results for the spin lattice with sandwich structure. (a) Specific heat. (b) Spin structure factor. (c) Resistance. (d) MR at different T's.

4. Conclusion

In conclusion, Monte Carlo simulations have been performed on classical Heisenberg spin lattices to qualitatively investigate the magnetoresistance effect. The resistor network is constructed based on the spin-dependent transport behavior. Not only the pure ferromagnetic and antiferromagnetic phases, but also several phase competitive cases have been studied, in some of which considerable values of magnetoresistance has been observed, accompanied by phase competitions (ferromagnetic versus paramagnetic, or ferromagnetic versus antiferromagnetic). The absence of colossal magnetoresistance in our simulation implies the essential role of charge ordered states (like the CE-type antiferromagnetic state) which exist in real manganites, but are not covered in the current pure spin model. Even so, our classical spin model provides an intuitive understanding on spin-dependent transport in magnetic systems, especially for those physical problems in large scale, since the more sophisticated quantum models (e.g., two-orbital double-exchange model with electron–phonon couplings) are usually limited to very small clusters.

References

[1] Žutić I, Fabian J and Sarma S D 2004 *Rev. Mod. Phys.* **76** 323
[2] Imada M, Fujimori A and Tokura Y 1998 *Rev. Mod. Phys.* **70** 1039
[3] Dagotto E, Hotta T and Moreo A 2001 *Phys. Rep.* **344** 1
[4] Dagotto E 2005 *Science* **309** 257
[5] Tokura Y 2006 *Rep. Prog. Phys.* **69** 797
[6] Zener C 1951 *Phys. Rev.* **81** 440
[7] Zener C 1951 *Phys. Rev.* **82** 403
[8] Goodenough J B 1955 *Phys. Rev.* **100** 564
[9] Millis A J, Littlewood P B and Shraiman B I 1995 *Phys. Rev. Lett.* **74** 5144
[10] Millis A J 1998 *Nature* **392** 147
[11] Dagotto E 2005 *New J. Phys.* **7** 67
[12] Shen J, Ward T Z and Yin L F 2013 *Chin. Phys. B* **22** 017501

[13] Aliaga H, Magnoux D, Moreo A, Poilblanc D, Yunoki S and Dagotto E 2003 *Phys. Rev. B* **68** 104405
[14] Şen C, Alvarez G and Dagotto E 2007 *Phys. Rev. Lett.* **98** 127202
[15] Yu R, Dong S, Şen C, Alvarez G and Dagotto E 2008 *Phys. Rev. B* **77** 214434
[16] Şen C, Alvarez G and Dagotto E 2010 *Phys. Rev. Lett.* **105** 097203
[17] Şen C, Liang S and Dagotto E 2012 *Phys. Rev. B* **85** 174418
[18] Chen L P, Ma Y B, Song X F, Lian G J, Zhang Y and Xiong G C 2008 *Chin. Phys. Lett.* **25** 3381
[19] Dong S, Yu R, Yunoki S, Liu J M and Dagotto E 2008 *Phys. Rev. B* **78** 064414
[20] Dong S, Yu R, Yunoki S, Liu J M and Dagotto E 2008 *Phys. Rev. B* **78** 155121
[21] Mayr M, Moreo A, Vergés J A, Arispe J, Feiguin A and Dagotto E 2001 *Phys. Rev. Lett.* **86** 135
[22] Caparica A A, Bunker A and Landau D P 2000 *Phys. Rev. B* **62** 9458
[23] Tsai S H and Landau D P 2000 *J. Appl. Phys.* **87** 5807
[24] Dong S, Zhu H, Wu X and Liu J M 2005 *Appl. Phys. Lett.* **86** 022501
[25] Dong S, Zhu H and Liu J M 2007 *Phys. Rev. B* **76** 132409
[26] Ju S, Cai T Y and Li Z Y 2005 *Phys. Rev. B* **72** 184413
[27] Ward T Z, Liang S, Fuchigami K, Yin L F, Dagotto E, Plummer E W and Shen J 2008 *Phys. Rev. Lett.* **100** 247204
[28] Yao X Y, Dong S, Zhu H and Liu J M 2005 *J. Appl. Phys.* **98** 093908
[29] Li X Q, Xu X G, Wang S, Wu Y, Zhang D L, Miao J and Jiang Y 2012 *Chin. Phys. B* **21** 107307